Terahertz Circular Variable Filters

E.N. Grossman [(1)], C.R. Dietlein [(1)], Arttu Luukanen [(2)]

[(1)] Optoelectronics Division, National Institute of Standards andTechnology
325 Broadway ,mailstop 815.04
Boulder, CO 80305, United States
Email: grossman@boulder.nist.gov, dietlein@boulder.nist.gov

[(2)] Millilab, VTT Information Technology
Espoo, Finland
Email: arttu.luukanen@vtt.fi

Abstract

We describe a novel class of millimeter-wave and terahertz monochrometers based on adiabatically tuned frequency-selective surfaces. They are analogous to the circular-variable filters commonly used in the infrared for low to moderate resolution spectroscopy, and are well adapted for hyperspectral imaging of explosives, bioagents, and other solid materials that display broad but distinct spectral features in the submillimeter wavelength band. Low-cost fabrication techniques based on copper-on-kapton "flex" circuitboard materials and patterning enable operation to approximately 800 GHz and coverage of areas greater than 0.5 x 0.5 m. Higher frequency operation can be obtained with wafer-based photolithography and standard micromachining techniques. Octave-band prototypes covering 110-220 and 220-440 GHz show resolving powers of >6, presently limited by beamsize in the measurement setup, and insertion loss <0.5 dB

Keywords: terahertz, millimetre-wave, monochrometer, filter, frequency-selective surface, hyperspectral

1. INTRODUCTION

Current interest in exploitation of the terahertz region of the spectrum is intense, and although originally stimulated by development of the time-domain spectroscopic (TDS) technique, it encompasses many technological approaches [1]. A large class of security applications relates to hyperspectral imaging, using the THz spectroscopic signatures of explosives [2] or bioagents [3, 4] to screen for these substances from a significant standoff distance and over an extended field-of-view. An important property of these signatures is that they are spectrally broad. This distinguishes these applications from more traditional THz spectroscopy focused on low-pressure molecular gases [5], for which high resolution techniques employing swept CW oscillators or heterodyne receivers are the most appropriate technologies.

One natural approach to low resolution hyperspectral imaging is use of a sensitive, broadband THz detector or detector array behind a THz monochromator. Broadband THz detector arrays can be realized cryogenically [6-8], although cost and system complexity are significant challenges in this case. There is also considerable effort underway to develop uncooled THz detector arrays [9] that would be suitable for such security applications; in this case sensitivity is the predominant challenge. In either case, a THz monochromator is required in front of the array to provide the spectral information.

Traditional approaches to a monochromator for the THz band would include fourier-transform interferometers (FTIR), diffraction gratings, and Fabry-Perot interferometers. All three are widely used at IR frequencies. FTIR's involve moving parts which must be accelerated and decelerated, which dramatically limits the speed of acquiring a spectrum, typically to a maximum of ~ 1 frame/s. Real-time (30 frames/s) spectroscopic imaging in particular is impossible. They are also relatively large, sensitive to misalignment, and expensive. Diffraction gratings use up one spatial dimension to obtain spectral information and are also large. Fabry-Perots, like FTIRs, require linear mechanical motion, and are therefore also slow and sensitive to misalignment. In summary, although all three approaches can provide resolving powers $f/\Delta f$ of several hundred or more, much higher than needed, all three are also much more complex and higher cost than is desirable.

On the other hand, another well known (almost antique!) infrared monochromator, the circular variable filter (CVF), is very simple and low-cost [10], and if adequate signal-to-noise is available from the broadband detector, it can operate at 30 spectra/s. It consists of a disk, rotated about its axis of symmetry, on which a bandpass interference filter is implemented using a stack of dielectric thin films. The thicknesses and spacings of the thin films vary with azimuthal position on the disk in such a way that the center frequency of the filter also varies continuously with azimuth. When configured with a fixed beam incident from one side of the CVF, a low cost monochromator is realized, yielding at least one complete spectrum every revolution. Unlike monochromators based on linear motion, real-time operation, ie. 30 spectral scans per second, is easily realizable. The infrared CVF cannot be directly scaled to the terahertz band however, because the dielectric thin films that form the basis of interference filters would need to be made impractically thick – tens or hundreds of microns, beyond the capabilities of ordinary thin film deposition techniques. However, the use of frequency-selective surfaces (FSS), i.e. periodic arrays of metallic shapes supported by a thin dielectric substrate, to perform filtering functions has been well known since FSS's were first invented [11, 12]. They can be configured to perform low-pass, high-pass, bandpass or bandstop functions [13],[14],[15].Their design and performance, particularly for reduction of radar cross-section at microwave frequencies (i.e. "stealth technology") is comprehensively reviewed in recent textbooks [16, 17]. They provide a simple and natural means of adapting the CVF to THz frequencies.

2. DESIGN AND FABRICATION

The basic principle of the THz CVF is illustrated in Fig. 1. Two basic geometries, which we refer to as "disk" and "drum" types, are possible. A frequency-selective surface (FSS) is constructed in which the dimensions of the unit cell are gradually tapered along a circular path, in such a way that the filter passband of the FSS also tapers gradually along this circular path. The preferred method of manufacture for the FSS is photolithographic patterning of very thin flex circuitboard (copper on kapton). The FSS is mounted on a suitable frame and the entire assembly rotated at a fixed angular velocity. A beam of terahertz radiation, fixed in space, is incident on the FSS. The output beam of radiation, which may either be transmitted or reflected depending on configuration of the FSS, (although only the transmission case is illustrated in Fig. 1) then comprises a filtered version of the input, with a filter passband that varies continuously in time. Thus a monchrometer is constructed that is extremely simple and may be constructed at very low cost. Its resolving power is determined by the FSS design and by the size of the incident beam. Despite the extraordinary simplicity of the THz CVF, the use of FSS's to perform the function of a monochromator, i.e. continuously variable filtering, does not seem to have been suggested before. Tapered periodic surfaces (TPS) have been introduced, but only for purposes of reducing diffraction near the edges of an FSS, thereby reducing the radar cross-section of objects such as airborne radomes that employ an FSS [18].

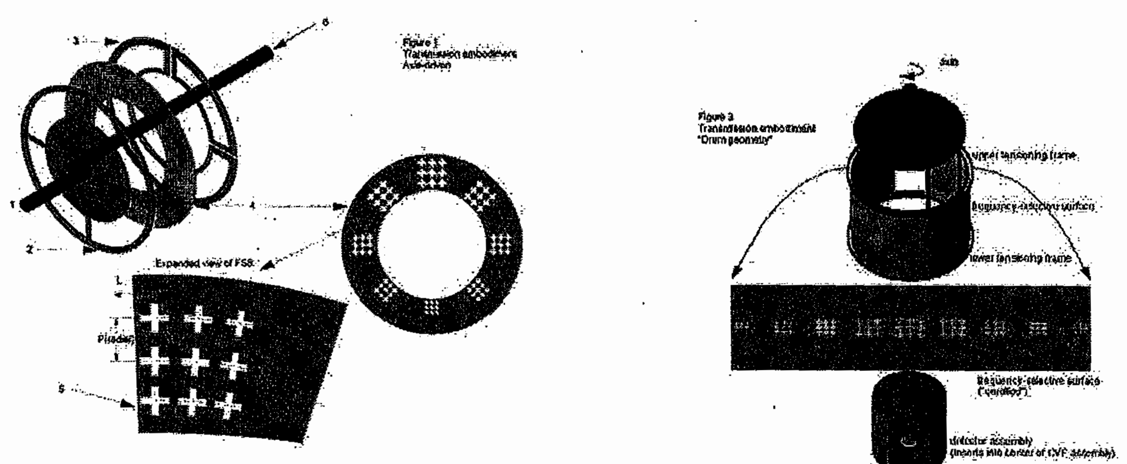

Figure 1. Basic design prinicple of the THz CVF, illustrated with simple crossed-slot FSS design. (Left) "disk" geometry in which the rotation axis is normal to the FSS, (right) "drum" geometry, in which the rotation axis is parallel to the FSS. In this case, the broadband detector array lies inside the FSS. Unit-cell dimensions for the crossed slot elements variy continuously along the circular rotation path.

2.1 Mathematical notation for FSS design:

The following notation will be used to describe the FSS design for the THz CVF :

- r, z, ϕ : cylindrical coordinates describing position in the FSS
- f, frequency
- $\lambda_0 = c/f$, free space wavelength (c is the free space velocity of light)
- $n = \sqrt{\varepsilon}$, substrate refractive index (square root of dielectric constant)
- t, substrate thickness

$L(\varphi)$, slot length as a function of azimuth
$P(\varphi)$, slot periodicity as a function of azimuth
$W(\varphi)$, slot width as a function of azimuth
L_1, P_1, W_1, slot length, periodicity, and width at the minimum wavelength
f_c, λ_c center frequency and center wavelength
T, transmittance of FSS

For disk-geometry FSS's, r and ϕ describe position on the FSS; for drum-geometry FSS's, z and ϕ describe the position. ϕ is azimuthal position, i.e. the direction of mechanical rotation, and the direction in which the center frequency varies.

2.2 Design implementation for first prototype:
For the first prototype, we have selected a center frequency profile described by

$$f_c(\varphi) = f_{\max} - \frac{(f_{\max} - f_{\min})}{\pi}\left|\phi - \pi\right| = \frac{c}{\lambda_c(\phi)} . \qquad (1)$$

Other f_c profiles may be used, and may be more suitable in particular applications. The above profile was selected because it has no discontinuities in $f_c(\varphi)$, eliminating fast transient signals in the output of a detector following the CVF, which could produce spurious artifacts in the resulting spectra. Moreover, since the FSS is rotated at a constant angular velocity, $a = \frac{d\varphi}{dt}$, this f_c profile ensures that, as a function of time, the frequency of maximum transmittance is a triangle wave. This makes signal-to-noise ratio uniform across an entire spectrum (since rms noise scales as the inverse square root of the integration time). It also makes deconvolution of the time sequence of data samples into a frequency spectrum more straightforward.

At the simplest level, varying the center frequency of the FSS according to a particular azimuthal profile, such as that of eqn. 1, is accomplished by directly scaling all lateral dimensions of the FSS unit cell proportionally to $\lambda_c(\phi)$, i.e. inversely with the center frequency. If the substrate thickness were sufficiently small, in practice less than $0.05\lambda/n$, then this simple scaling would be exact, and the prescriptions $L(\phi) = L_1 \frac{\lambda_c(\phi)}{\lambda_c(\min)}$, $W(\phi) = W_1 \frac{\lambda_c(\phi)}{\lambda_c(\min)}$, $P(\phi) = P_1 \frac{\lambda_c(\phi)}{\lambda_c(\min)}$, along with eqn. 1, would constitute a complete design specification. However, the preferred method of manufacturing the THz CVF uses conventional flex circuitboard, i.e. copper on a kapton substrate, as the starting material, and the thinnest flex presently available is 25 micron thick. In this case, the shortest wavelength for which the $t < 0.05\lambda/n$ criterion is valid is 920 micron, corresponding to 330 GHz. In order to realize the preferred $f_c(\varphi)$ profile given by eqn. 1, at higher frequencies, corrections must be made for the finite and fixed substrate thickness.

2.2.1 Correction for fixed and finite substrate thickness
For crossed-slot elements, and in the limit of an infinitesimally thin substrate, the resonant slot length is $L = \lambda/2$, while in the limit of a thick substrate, (dielectric half-space), the resonant slot length is reduced by the square-root of the average dielectric constant, i.e. $L = \frac{\lambda}{\sqrt{2(\varepsilon+1)}}$, the "quasi-static" value. The transition between these two extremes is illustrated in the data of MacDonald [19], which describes the dependence of resonant length on substrate thickness and dielectric constant. That data may be approximated by an exponential transition, yielding

$$L = (.5\lambda_c)\left[(1-.27)+.27\exp(-t/.035\lambda_c)\right] \qquad (2)$$

where the values .27 and .035, obtained from fits to MacDonald's data, apply to mylar substrates ($n = \sqrt{\varepsilon} = 1.74$). This is only slightly different from the presently used substrate material, kapton (n=1.84)., Given the desired azimuthal profile of resonant wavelength eqns. 1 and 2 then provide the full design specification for slot length, $L(\varphi)$.

2.2.2 Radial variation and effect of grating lobes

For the geometry shown in Fig. 1a, in which the circular path of rotation lies in the plane of the FSS, it is clear that some of the element dimensions (L,P,W) must vary with r, as well as with φ, even though only the latter variation is needed to perform the monochromator function. This is simply because circular paths at larger radius have larger circumference. Unless additional "spokes" in the FSS are inserted at larger radii, either the slot lengths or the (azimuthal) distances between slots, and therefore P, must increase to fill the larger circumference. For FSS's based on crossed slots, the slot length primarily determines the center frequency f_c, the slot width primarily affects the bandwidth or quality factor (Q) of the passband, and the periodicity primarily affects the onset of grating lobes. Since the function of the CVF relies on azimuthal, but not radial, variation of f_c, we chose to hold L, and thus f_c, constant as a function of radius, and allow P to increase at large radius. This implies that grating lobe behavior varies with radial position. Clearly, this effect is mitigated by making the active annulus (the area of the FSS intercepted by the beam) as fractionally narrow as possible, i.e. by minimizing $(r_{\max} - r_{\min})/(r_{\max} + r_{\min})$, though this involves a tradeoff with physical size of the CVF. The angle of the grating lobes and the frequency of their onset are determined by the periodicity of the FSS through the grating equation:

$$\sin\theta_i + \sin\theta_g = \frac{n\lambda}{P} \tag{3}$$

Thus, for operation at normal incidence ($\sin\theta_i = 0$), as illustrated in Fig. 1, grating lobes first appear when the period equals the wavelength. On the other hand, the resonance condition is that the slot length be half the wavelength. Thus it is impossible to obtain a completely grating-lobe free stopband that extends more than one octave in frequency above the passband. A crossed-slot CVF can therefore be straightforwardly designed to cover one octave, since at the azimuthal location corresponding to $f_c(\min)$, signals at $f_c(\max)$ will still be rejected. However, for larger fractional frequency coverage, incident signals at $f_c(\max)$ will, when the wheel is oriented for $f_c(\min)$, be scattered into non-specular angles (initially near grazing). With appropriate baffling, this can be tolerated, so CVF's with fractional frequency coverage greater than an ocatve certainly are feasible. However, the baffling required for grating lobe rejection is completely dependent on detailed system geometry. We chose for the initial prototype to confine ourselves to one octave.

2.3 Fabrication and mounting details:

Prototypes have been constructed for the 110-220 GHz and 220-440 GHz bands. Fig. 2 shows a photograph of the

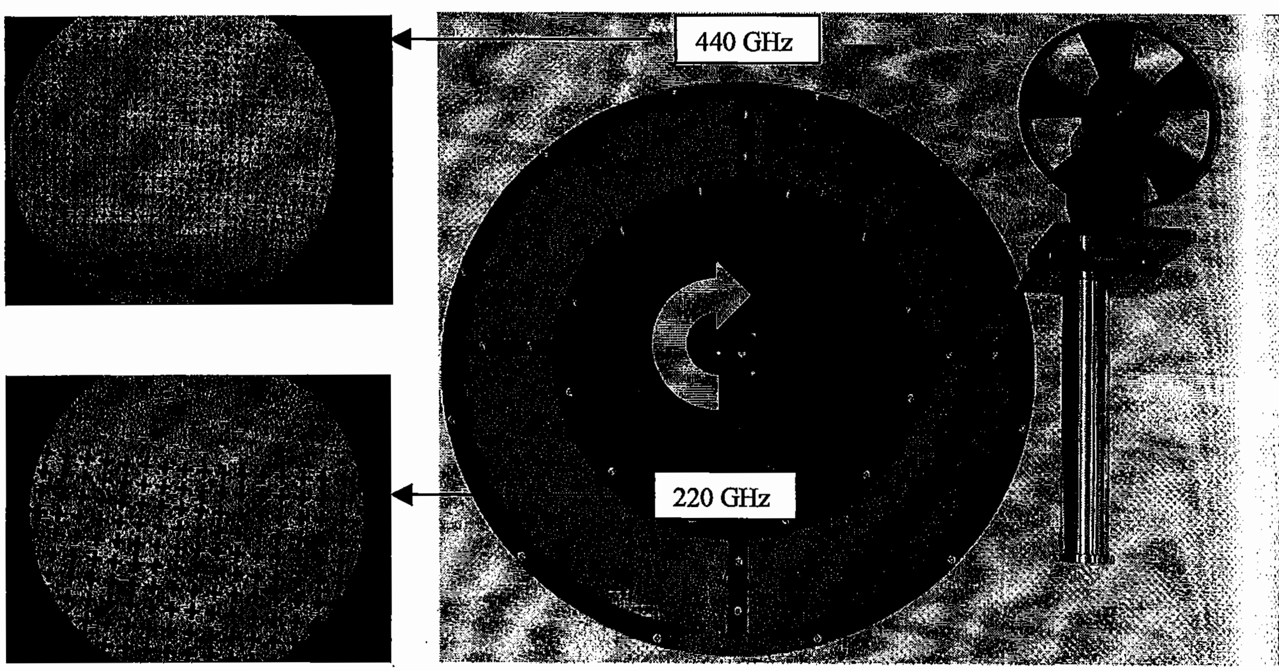

Fig. 2 Photograph of a 220-440 GHz CVF implemented on 25 μm thick Cu on kapton "flex" circuitboard.

higher frequency prototype. One of the primary advantages of the THz CVF is its ability to be manufactured at extremely low cost. The raw material used in our prototype is copper-on-kapton laminate, with kapton thickness of 25 μn and Cu thickness of 18 μm. Such material is now manufactured in large volume as "flex" circuitboard, and used in a wide variety of electronic applications, so its cost is remarkably low (often under 100 USD per square meter). Thin kapton is highly transparent at THz frequencies, while the copper is an exceedingly good conductor. Likewise, the material can be patterned by the same lithographic processes used for manufacturing flex circuitry, also at remarkably low cost. Typically, minimum linewidths of ~50 μm would imply an upper frequency limit of approximately 1 THz. (The most primitively defined cross consists of two bars, each three linewidths long. Setting this length equal to a half wavelength results in a short wavelength limit approximately six times the minimum linewidth.) The greatest challenge in using the flex material lies in mounting it in such a way that it remains flat and taut even while the assembly is rotated at high speed. Clearly, wafer-scale microlithographic fabrication on Si_3N_4 micromachined membranes could be used if higher frequency operation were necessary.

In the disk geometry of Fig.1 that was implemented in our prototype, the planar FSS is mounted on a frame consisting of a solid circular disk, in which an annular slot has been cut out. The FSS mounts in this annular slot and the beam passes through the FSS. In order to support the outer rim of the disk, to which the outer edge of the FSS is affixed, spokes must be retained in the circular disk, which interrupt the FSS and the filtered beam. The FSS is mounted by squeezing it between the main disk and a retaining ring. A "stretcher" is then bolted to the assembly, which presses against the FSS in the third dimension in order to make the surface taut. In our prototype, the retaining ring and the stretcher are both divided into quadrants, each lying between 2 of the spokes. Alternatively the FSS could be constructed in the form of a uninterrupted circular disk, stretched upon a narrow circular frame. In this case however, the entire assembly cannot be supported by an axle on the center of rotation because the FSS is too flimsy to support the circular frame. The circular frame would therefore have to be supported by 3 or more bearings on its perimeter. As illustrated in Fig. 2, the completed CVF assembly was mounted on a commercial optical chopper. The original chopper blade was retained, and, with the built-in optical interrupter circuit, provided a trigger signal for data acquisition.

3. MEASUREMENTS

Fig. 3 shows a series of optical transmittance measurements that characterize the lower frequency CVF, taken using a CW Gunn oscillator with external frequency doubler as a source. Each trace, corresponding to a particular frequency, has been normalized to its peak. The CVF was rotated at ~ 2Hz for these measurements, yielding 4 spectra/sec. The absolute transmittance was measured separately and found to exceed 90 % (at the azimuth of peak transmittance) for all frequencies. The beam was feedhorn-coupled at both source and detector. The directly measured Q values (f/Δf) are approximately 6. However, the intrinsic resolving power of the FSS somewhat exceeds this value, since it was realized after the measurements were complete that the ~40 mm beamsize is enough to significantly broaden the observed peaks.

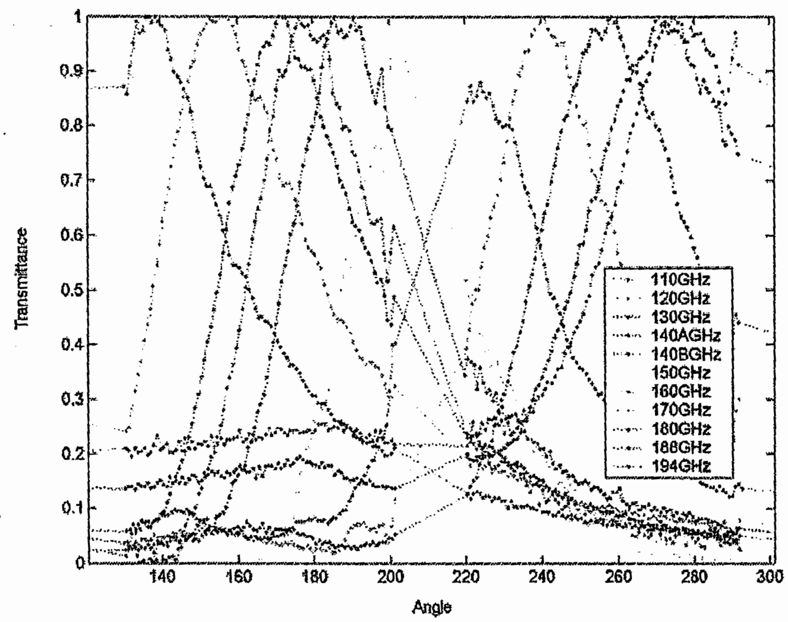

Fig. 3. Measured transfer function (transmittance as a function of angle and frequency) of the 110-220 GHz CVF prototype. Width of the peak was limited by beamsize in the particular measurement setup.

CONCLUSION

We have described a monochrometer, analogous to an IR CVF, that is well suited to low-resolution spectroscopy in the 100 GHz – 1 THz range. It uses a frequency-selective surface (FSS) based on an array of crossed-slot antennas. The array's geometric parameters vary smoothly around the perimeter of an annular window in such a way as to produce a bandpass filter whose center frequency tunes linearly with angle, as the annulus is rotated around its center. Once calibrated using monochromatic sources, the monochrometer can be applied in conjunction with a high sensitivity detector and a heated (or cooled) background to obtain transmission or reflection spectra of unknown samples. The spectral resolution is well matched to the broad THz spectral features of explosives and bioagents that are the focus of intense current interest.

REFERENCES

[1] D. L. B. Woolard, E.R., Pepper, M., Kemp, M. , "Terahertz frequency sensing and imaging: a time of reckoning future applications?," *Proceedings of the IEEE*, vol. 93, pp. 1722-1732, 2005.

[2] Y. C. Shen, T. Lo, P. F. Taday, B. E. Cole, W. R. Tribe, and M. C. Kemp, "Detection and identification of explosives using terahertz pulsed spectroscopic imaging," *Applied Physics Letters*, vol. 86, pp. 241116, 2005.

[3] T. Globus, Ramakrishnan Parthasarathy, Tatyana Khromova, Dwight Woolard, Nathan Swami and J. W. Andrew J. Gatesman, "Optical characteristics of biological molecules in the Terahertz gap," *Proc SPIE*, vol. 5584, 2004.

[4] D. L. Woolard, E. R. Brown, A. C. Samuels, J. 0. Jensen, T. Globus, B. Gelmont and M. Wolski, "Terahertz-Frequency Remote-Sensing of Biological Warfare Agents," *IEEE MIT-S Digest*, pp. 763-766, 2003.

[5] I. Medvedev and F. C. D. L. Markus Behnke, "Fast analysis of gases in the submillimeter/terahertz with ``absolute" specificity," *Applied Physics Letters*, vol. 86, pp. 154105, 2005.

[6] A. Luukanen, Miller, A.J., Grossman, E.N., "Passive Hyperspectral Terahertz Imagery for Security Screening using a Cryogenic Microbolometer," *Proc. SPIE*, vol. 5810, 2005.

[7] A. Luukanen, Hadfield, R.H.,Miller, A.J.,Grossman, E.N., "A superconducting antenna coupled microbolometer for THz applications," *Proc. SPIE*, vol. 5411, 2004.

[8] W. S. Holland, E. I. Robson, W. K. Gear, C. R. Cunningham, J. F. Lightfoot, T. Jenness, R. J. Ivison, J. A. Stevens, P. A. R. Ade, M. J. Griffin, W. D. Duncan, J. A. Murphy, and D. A. Naylor, "SCUBA: a common-user submillimetre camera operating on the James Clerk Maxwell Telescope," *Monthly Notices of the Royal Astronomical Society*, vol. 303, pp. 659-672, 1999.

[9] C. M. Stickley and M. E. Filipkowski, " MIcroantenna Arrays: Technology and Applications (MIATA)--an overview " *Optics and Photonics for Counterterrorism and Crime Fighting. Edited by Donaldson, Tim P.; Lewis, Colin. Proceedings of the SPIE, Volume 5619, (2004)*, vol. 5619, pp. pp. 47-58 2004.

[10] C. Wyatt, "Infrared spectrometer: liquid-helium-cooled rocketborne circular-variable filter," *Appl. Opt.*, vol. 14, pp. 3086-3091, 1975.

[11] B. A. Munk, "Periodic Surface for Large Scan Angles." U.S. Patent 4,789,404, 1974.

[12] B. A. Munk, "Space Filter." U.S. Patent 4,125,841, 1977.

[13] T. Timusk, and P. L. Richards, "Near millimeter wave bandpass filters," *Appl. Opt.*, vol. 20, pp. 1355, 1981.

[14] D. Porterfield, J. Hesler, R. Densing, E. Mueller, T. Crowe, and R. Weikle II, , "Resonant Metal-mesh Bandpass Filters for the Far-infrared," *Appl. Optics*, vol. 33, pp. 6046-6051, 1994.

[15] O. S. Karl D. Moeller, Haim Grebel, and Kenneth P. Stewart, "Inductive cross-shaped metal meshes and dielectrics," *Appl. Opt.*, vol. 41, pp. 3919, 2002.

[16] B. A. Munk, *Frequency Selective Surfaces, Theory and Design*. New York: John Wiley, 2000.

[17] B. A. Munk, *Finite Antenna Arrays and Frequency Selective Surfaces*. New York: John Wiley, 2003.

[18] E. K. English, and Leeper, W.J., "Periodic Surfaces for Selectively Modifying the Properties of Reflected Electromagnetic Waves." U.S. Patent 5,606,335 1997.

[19] M. E. MacDonald, A. Alexanian, R. A. York, Z. Popovic, and E. N. Grossman, "Spectral Transmittance of Lossy Printed Resonant-Grid Terahertz Bandpass Filters," *IEEE Trans. Microwave Theory and Techniques*, vol. 48, pp. 712-718, 2000.